

PARASITIC CONES IN THE THARSIS VOLCANIC PROVINCE ON MARS: IMPLICATIONS FOR ITS RECENT MAGMATIC PLUMBING SYSTEM

B. Pieterek¹, J. Ciazela², D. Mège², P.-A. Tesson², M. Ciazela², J. Gurgurewicz², A. Lagain³, and A. Muszyński¹
¹Institute of Geology, Adam Mickiewicz University, ul. Bogumiła Krygowskiego 12, 60-680 Poznan, Poland (barpie@amu.edu.pl), ²Space Research Centre, Polish Academy of Sciences, ul. Bartycka 18A, 00-716 Warsaw, Poland, ³Space Science and Technology Centre, Curtin University, Kent Street, Bentley, Perth, Western Australia 6102, Australia.

Introduction: Although Tharsis is the largest volcanic province on Mars, the origin of numerous small volcanic cones in this area is not yet fully explained. On the one hand, their genesis may be related to the evolution of larger volcanic edifices, such as Olympus Mons or the Tharsis Montes. Bleacher et al. [1] have observed structural relationship of parasitic cones and inherent lava flows related to the Pavonis Mons indicating coeval development of the main edifice and small cones. On the other hand, due to the widespread distribution of the small cones, some researchers suggest, that they have no direct link to the large volcanoes and try to relate small cones to the fault systems [2]. Characterizing the system of small volcanic cones in terms of space and time is essential to understand Tharsis magmatic plumbing complex. In this study, we analyze the spatial distribution, surface age, as well as orientation of volcano summit craters (Fig. 1A) or central fissure vents (Fig. 1B) to determine whether or not they are geologically associated with the major Tharsis volcanoes.

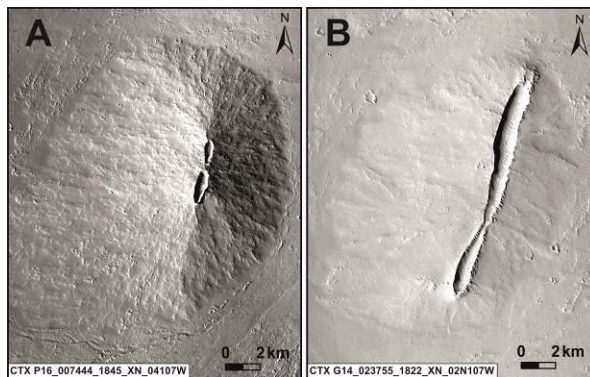


Figure 1. Examples of parasitic cones with measured elongated volcanic summit crater (A), and a central fissure vent (B).

Method: We mapped the parasitic cones of Tharsis, determined the orientation of their elongated craters or central fissure vents, and dated some of the volcano flanks (Figs. 2 and 3). The parasitic cones were mapped combining imagery from the Thermal Emission Imaging System (THEMIS) of Mars Odyssey (MO) (spatial resolution of ~100 m/pixel) for first identification and the Context Camera (CTX) of Mars Reconnaissance Orbiter (MRO) (6 m/pixel) for de-

tailed mapping. In some cases, we analyzed images from the High Resolution Imaging Science Experiment (HiRISE; 25-32 cm/pixel) of MRO to distinguish the smallest parasitic cones (1-2 km in diameter) and measure the orientation of summit elongated craters or central fissure vents. The orientations were plotted on the rose diagrams (Fig. 3) using Stereonet 10.2. ArcMap was used for mosaicking and mapping.

Selected parasitic cones (Fig. 3) were dated using crater counting (>100 m in diameter) with the ArcGIS extension CraterTools2.1 [3] on the CTX mosaic. Crater statistics and derivation of crater model ages, including errors (Figs. 2 and 3), was carried out with CraterStats II [4] by applying the Hartmann's (2005) chronology system [5,6].

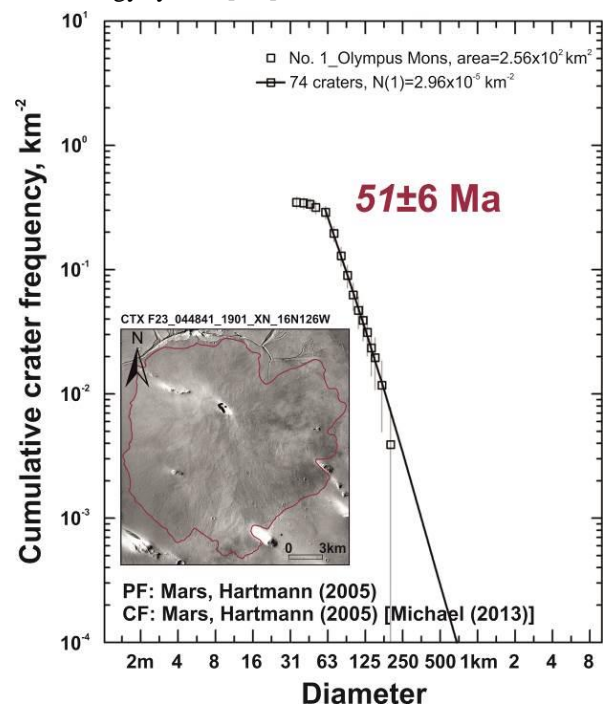
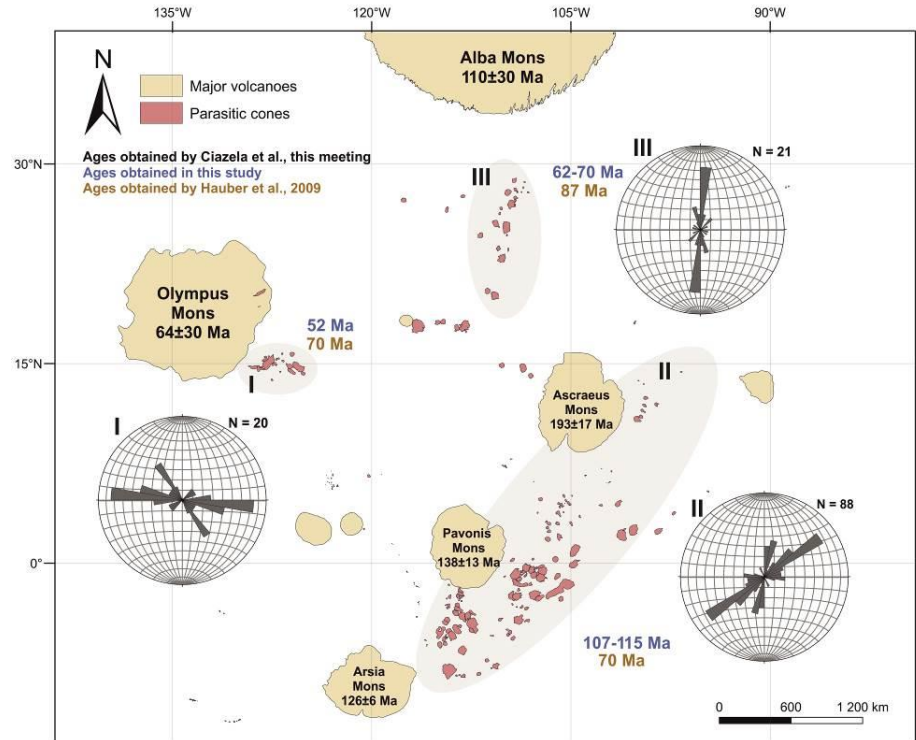


Figure 2. Example of dated parasitic cone and chronology curve produced by CraterStats.

Results and Discussion: We mapped 302 parasitic cones of diameter >1 km. They are unevenly distributed across the Tharsis province, with most of them occurring roughly parallel to the Tharsis Montes (Fig. 3). Based on volcano geographic distribution and measured orientations of elongated summit craters and

Figure 3. Map of major volcanoes (beige) and parasitic cones (red) in the Tharsis volcanic province. The parasitic cones are clustered in three major groups (1) near Olympus Mons (2) near Tharsis Montes, and (3) located at the south from Alba Mons. The rose diagrams show orientations of volcano summit craters or central fissure vents, and N-number correspond to the number of volcanic structure in each group.



central fissure vents we distinguish three major groups related to 1) Olympus Mons (with orientations of ~N100E) 2) Tharsis Montes (~N055E), and 3) Alba Mons (~N005E) (Fig. 3). The three identified groups represent distinct episodes of volcanism associated with different major volcanoes. To further investigate the connection between parasitic cones and the main volcanoes, we dated 6 parasitic cones in the identified subprovinces, as well as the most recent caldera activity of the major volcanoes. All results are presented in the Table 1.

The parasitic cones reveal similar ages as the adja-

Table 1. Age comparison between the three sets of parasitic cones (Fig. 3) and the related major volcanoes.

Subprovince	Age (Ma)		Coordinates	
	Major volcano	Parasitic cones	Parasitic cones	
Olympus Mons	64±30	51±6	15°45'52"N	125°59'36"W
		52±12	14°53'16"N	126°17'43"W
		126±6	0°19'56"N	106°12'29"W
Tharsis Montes	138±13	107±28	0°55'41"S	107°49'33"W
		115±13	24°40'35"N	111°46'28"W
		193±17	23°44'04"N	110°25'42"W
Ceraunius Fossae	110±30	62±9	111°46'28"W	23°44'04"N
		70±20	110°25'42"W	110°25'42"W

cent feeding volcanoes. For example, the age of the last activity for Olympus Mons found to be 64 Ma [7], against ~52 Ma for the parasitic cones (Fig. 3). Hauber et al. [8] found a consistent ~70 Ma age for larger number of parasitic cones in the Olympus Mons group.

Conclusions: The obtained distribution of parasitic cones, along with their alignment and ages allowed us to distinguish three distinct systems related to 1) Olympus Mons, 2) Tharsis Montes, and 3) Alba Mons. Because both the small and the corresponding major volcanoes are relatively young (52–193 Ma), they reflect major features of the latest magmatic plumbing system, perhaps currently dormant [7]. We conclude that recent or current major magma reservoirs may be present below Olympus Mons, Tharsis Montes, and perhaps Alba Mons, with auxiliary magmatic activity concentrating along the interconnecting system of N-S (N005E), W-E (N100E) and SW-NE (N055E) trending fissures.

References: [1] Bleacher J. E. et al. (2007) *J. Geophys. Res. Planets*, 112, 1–15. [2] Hauber et al. (2009) *JVGR*, 185, 69–95. [3] Kneissl T. Å. et al. (2011) *Planet. Space Sci.*, 59, 1243–1254. [4] Michael G. G. and Neukum G. (2010) *EPSL*, 294, 223–9. [5] Hartmann W. K. (2005) *Icarus*, 174, 294–320. [6] Michael G. G. (2013) *Icarus*, 226, 885–890. [7] Ciazela J. et al. (2019) *LPSC 50*, 1364. [8] Hauber E. et al. (2011) *Geophys. Res. Lett.*, 38, 1–5.